

## Original Paper

# Effect of Nano-Silica on The Thermo-Physical Properties of the Thermal Eutectic $(\text{Na}_{0.6}\text{K}_{0.4})\text{NO}_3$ System

H. I. ElSaeedy<sup>1</sup>, A. A. S. Al Ahmari<sup>2</sup>, K. F. Abd El-Rahman<sup>3\*</sup> & S. Taha<sup>4</sup>

<sup>1</sup> Department of Physics, Faculty of Science for Girls, King Khalid University, P. O. Box 9004, Abha, Saudi Arabia

<sup>2</sup> Department of Physics, College of Arts and Sciences, King Khalid University, P. O. Box 900, Mahayel Asir, Saudi Arabia

<sup>3</sup> Department of Physics, Faculty of Education, Ain Shams University, Cairo, Egypt

<sup>4</sup> Department of Physics, Faculty of Science, Fayoum University, Fayoum, Egypt

\* K. F. Abd El-Rahman, elrahman100@gmail.com

Received: March 28, 2020

Accepted: April 9, 2020

Online Published: May 26, 2020

doi:10.22158/ees.v3n1p59

URL: <http://dx.doi.org/10.22158/ees.v3n1p59>

### Abstract

*Here, we investigate the effect of adding nano-silica particles on the thermo-physical properties of the  $(\text{Na}_{0.6}\text{K}_{0.4})\text{NO}_3$  based thermal energy storage systems. Five different systems tagged as  $M_{00}$ ,  $M_{01}$ ,  $M_{02}$ ,  $M_{03}$  and  $M_{04}$ , with different nano-silica percentage of 0, 1, 2, 3, and 4 wt%, respectively, were prepared. Various experimental techniques were employed to study the thermo-physical properties of the systems during (solid-solid) phase  $P_1$ , (solid-liquid) phase  $P_2$  and (liquid-solid) phase  $P_3$ , and to clarify the effect of nano-silica on the thermal energy storage efficiency during both charging and discharging processes. According to the Differential Scanning Calorimeter (DSC) thermal analysis, it was found that the system  $M_{02}$  whose nano-silica addition rate of 2 wt%, has the most favorable thermal characteristics (i.e., highest specific heat and lowest enthalpy change). Moreover, the addition of 2 wt% represents the optimum distribution of nano-silica inside the principal base system  $M_{00}$ . This leads to an improvement in the porosity of the system due to the degree of homogeneity caused by the thermophoresis effect distribution, the high surface area of the nano-silica with the activity of the  $M_{00}$  matrix alongside the degree of the alkalinity of nano-silica. Besides, the electric conductivity measurements showed that the 2wt% percentage is the optimum one for thermal energy storage systems.*

### Keywords

*phase change material, thermal storage, nano silica, calorimetry*

## 1. Introduction

Thermal energy storage systems can be classified into sensible heat storage, latent heat storage and thermo-chemical heat storage. Latent heat storage systems use the Phase Change Materials (PCMs) as thermal energy storage media, where the thermal energy is stored or released during the material phase change transition processes. Phase Change Materials (PCM) have been widely used for the thermal storage systems due to their capability of storing and releasing large amounts of energy within a small PCM volume, a moderate temperature variation and prolong the charging and discharging period. Additionally, significant attention has been given to using salts as a phase change storage media (using encapsulation and otherwise) (Goswami et al., 1990, pp. 257-262; Xu et al., 2015, pp. 286-307; Gaosheng et al., 2018, pp. 1771-1786; Hassan et al., 2019, pp. 491-523). Moreover, several mixtures of alkali nitrates and nitrites have been used as a heat transfer medium because of its low cost and good compatibility with common structural materials (Borul et al., 1954, pp. 233-238). The  $\text{NaNO}_3\text{-KNO}_3$  system is one of the most extensively investigated binary inorganic salt systems (Voskresenskaya et al., 2017, pp. 431-437; Silverman et al., 1977, pp. 1-26; Kamimoto et al., 1981, pp. 319-331; Kearney et al., 2003, pp. 170-176; Zhang et al., 2003, pp. 441-446; Berg et al., 2004, pp. 2224-2229; Villada1 et al., 2014, pp. 622-625; Lin et al., 2018, pp. 685-708). The PCM's low thermal energy storage efficiency remains, however, a big challenge for researchers. The PCM's thermal performance is positively correlated with three different parameters, the thermal conductivity coefficient, area for heat transfer, and the heat transfer temperature difference. Accordingly, the thermal performance can be enhanced by; enhancing the thermal conductivity, extending the heat transfer area, and improving the uniformity of heat transfer processes (Tao et al., 2018, pp. 245-259). The thermal conductivity can be enhanced by using additives with high thermal conductivity coefficient. The high thermal conductivity carbon-based, metal- fillers, porous materials, and nano-particles are commonly used as additives to enhance the thermal conductivity of the PCM (Lin et al., 2018, pp. 2730-2742). Using of the metal-based porous material, such as metal foam enhances heat transfer by reducing the cell size leading to the large contact surface area. In this case, the scattered air within the pores expands significantly to cause the ejection restriction of the phase transformation for the PCM during the actual operation at elevated temperatures (Wu et al., 2011, pp. 1371-1380). Using metal fillers led to a reduced discharging time and significant weight and cost to the thermal storage systems as well (Farid et al., 2004, pp. 1597-1615). In addition, corrosion could appear when using salts as PCM (Joel, 2008; Dorete et al., 2012, pp. 13-25; Grant, 2002, pp. 1-34). Also the addition of graphite to the binary thermal storage system leads to enhance the thermal conductivity coefficient and reduced the total latent heat (Xiao et al., 2015, pp. 272-284; Berg et al., 2004, pp. 2224-2229; Xiao et al., 2014, pp. 52-58; Zhao et al., 2014, pp. 272-277; Lopez et al., 2010, pp. 1586-1593). For nano-enhanced PCM material, the thermal conductivity depends not only upon the nano particle's concentration, the particle size and shape, but also on the base PCM material (Chieruzzi et al., 2013, pp. 448-456; Dudda et al., 2013, pp. 37-42; Leong et al., 2019, pp. 18-31; Jeyaseelan et al., 2019, pp. 235-242). In contrast to previous studies,

which addressed the impact of nano-particle on the thermal performance of PCM thermal storage material, the current study is devoted to investigate the effect of nano silica on both the thermal and the physical properties of the binary molten salt  $0.6\text{NaNO}_3\text{-}0.4\text{KNO}_3$ . Phase Change Materials (PCMs) based on latent heat energy storage techniques over a nearly isothermal temperature range using Paraffin Wax Nano composite Based on Carbon-Coated Aluminum Nano particles have been regarded (Chen et al., 2017, pp. 12603-12609). The thermal stability of paraffin wax was improved by the shape stabilization with 10 wt% of carbon nano tubes (Fredri et al., 2017, pp. 405-420). They mentioned that the modified paraffin wax is a promising strategy to meet the highly efficient thermal management system for electric vehicles.

## 2. Method

The binary salt was prepared by mixing 60% of  $\text{NaNO}_3$  with 40% of  $\text{KNO}_3$  by weight, in its solid form; these salts nitrates are ultra-pure from Aldrich Company. The mixture heated up to  $350^\circ\text{C}$  to achieve a complete melting for this mixture; the system was then cooled at room temperature. This system represents the eutectic system  $(\text{Na}_{0.6}\text{K}_{0.4})\text{NO}_3$ , and denoted in this work as  $M_{00}$  system. The solid binary salt was then milled to powder, and the nano-silica was dispersed into four concentrations: 1, 2, 3 and 4 wt% in the solid binary nitrate  $(\text{Na}_{0.6}\text{K}_{0.4})\text{NO}_3$  system separately to get  $M_{0x}$  ( $x=1, 2, 3,$  and  $4\%$ wt.) systems. The binary system and the nano-silica particles were dispersed in 20 ml of distilled water by ultrasonic mixing for 2 hours using MXBAOHENG Ultrasonic Homogenizer FS-T Series with nominal frequency of 20 kHz. The solutions were stirred by the strong ultrasonic homogeneous instrument for 2 hours, afterwards, the water solutions were heated at  $150^\circ\text{C}$  on a hot plate to fully remove the water for at least 1 hour (Shin et al., 2011, pp. 1064-1070).

By grinding the dried composites, samples were obtained, after the operation process for all samples, they were immediately used for thermal, electrical, structure and electron macroscopic analysis, to identify the effect of the nano-silica on the thermo-physical properties for the  $(\text{Na}_{0.6}\text{K}_{0.4})\text{NO}_3$ , which is representing the thermal storage media.

## 3. Result

### 3.1 DSC Measurements

The DSC thermo grams measurements for  $M_{00}$  and  $M_{0x}$  ( $x=1, 2, 3, 4$  wt%) systems have been carried out during heating and cooling. The DSC measurements were performed by using SHIMADZU DSC-60 plus series equipment. Figure 1 shows the thermo-grams for the base matrix ( $M_{00}$ ) as representative example. The figure indicates to the existence of three peaks. The first broad peak located at  $\approx 125^\circ\text{C}$ , is mainly due to the solid-solid phase transition ( $P_1$ ). This phase is related to the change in the specific heat (sensible heat storage) and the transition from the displacive type modified by orientation switching (Bauer et al., 2010, pp. 272-278; Al Sharhani, 2016; Hatakeyama et al., 1989, pp. 327-335).

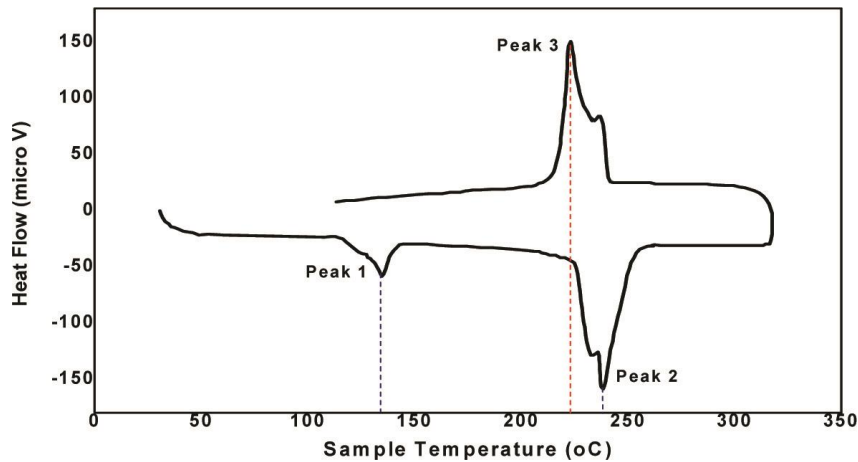


Figure 1. The DSC Thermo-Grms for  $M_{00}$  System

While the second endothermic peak located at  $\approx 234^{\circ}\text{C}$ , is related to the melting point of the  $M_0$  system, i.e., the phase change from solid-liquid phase ( $P_2$ ). The third exothermic peak at  $\approx 223^{\circ}\text{C}$  represents the phase change from liquid-solid phase ( $P_3$ ), i.e., the solidification process. The same three peaks appeared with the thermograms measurements of the samples  $M_{0x}$  ( $x=1, 2, 3, 4$  % wt.). The variations in the thermal parameters, such as the enthalpy, transition point, and peak position have been studied for all samples. For example, the specific heat of the sample can be determined from the relation (Hatakeyama et al., 1989, pp. 327-335):

$$C_{px} = \left(\frac{I_x}{I_s}\right) \left(\frac{M_s}{M_x}\right) C_{ps} \quad (1)$$

Where  $I_x$  is the peak height of the sample,  $I_s$  is the height of the standard material from the zero line of the starting of the equipment (DSC),  $M_s$  is the mass of the standard material ( $\text{Al}_2\text{O}_3$ ),  $M_x$  is the mass of the sample and  $C_{ps}$  is the specific heat of the standard material.

Also, the activation energy for all phases ( $P_1$ ,  $P_2$  and  $P_3$ ) at any system by using the modified Kissinger equation (Rysava, 1987, pp. 1015-1021):

$$\ln(\Delta Q) = G - \frac{Eg}{kT} \quad (2)$$

Where different heights corresponding to different temperatures for each peak have been obtained. The extracted data were used to plot as  $\ln(\Delta Q)$  and  $1/T$  according to the equation and hence to get the activation energy.

All the thermal kinetic parameters for the  $M_0$  system are shown in Figure2 (a and b) as representative example. It can be easily seen that the transition temperature does not nearly change in the all phases ( $P_1$ ,  $P_2$  and  $P_3$ ) with the increasing the concentration of the nano-silica in the  $M_{0x}$  system. These results suggest that the nano-silica inside the  $M_{0x}$  system having a uniform distribution and a homogeneous dispersion. This leads the  $\text{SiO}_2$  (nano-silica) takes part in the network structure as a network former (Chieruzzi et al., 2013, pp. 448-456).

The variations in entropy ( $\Delta H$ ), the peak height, the transient temperature ( $\Delta T$ ) and the transient time ( $\Delta t$ ) with the concentration of the nano-silica for all phases ( $P_1$ ,  $P_2$  and  $P_3$ ) are mainly related to the distribution effect on the interaction potential of  $\text{Na}^+$  and  $\text{K}^+$  ions around the  $(\text{NO}_3)^-$  group in the  $M_{0x}$  system (Taha et al., 1994, pp. 217-226). For the entropy ( $\Delta H$ ) and the peak height, it is clear from the figure that there is a minimum value corresponding to concentration value  $x \approx 2\%$  of nano-silica. This means that the  $M_0$  system at that percentage become more stable than that at any other concentration of nano-silica, due to the stability of the thermodynamics function (Thirriwg, 2006, pp. 113-121).

The minimum value of ( $\Delta H$ ) at this concentration ( $x \approx 2\%$  of nano-silica) indicates that the system has a higher ordered and mechanical stability than other any concentration.

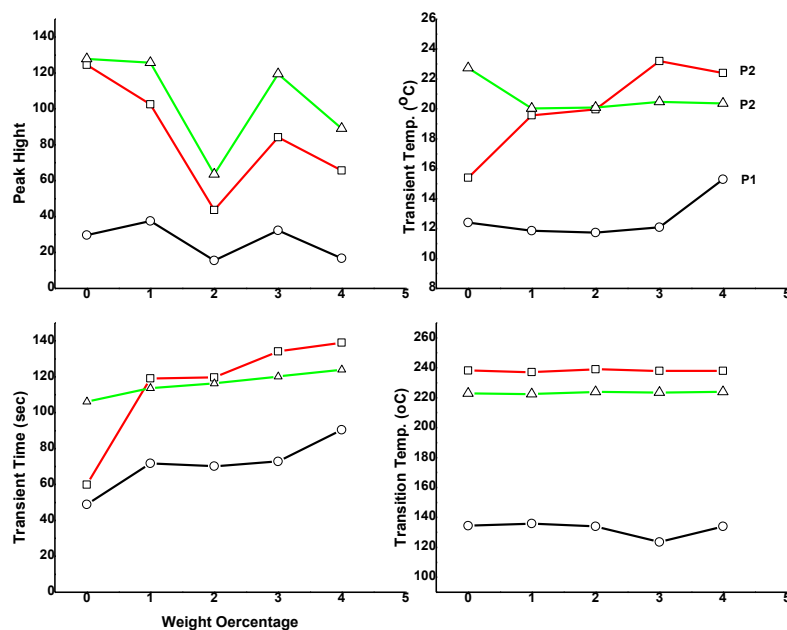


**Figure 2. The Thermal Kinetic Parameters (Peak Height, Transient Temperature, Transient Time and Transition Temperature) for  $M_{0x}$  System with Different Concentration of Nano Silica**

This is supported by the variation of the transient temperature ( $\Delta T$ ) and the transient time ( $\Delta t$ ), where ( $\Delta T$ ) and ( $\Delta t$ ) which does not nearly change in the concentration range  $1\% \leq x \leq 2\%$  for each phase ( $P_1$ ,  $P_2$  and  $P_3$ ). These results are mainly related to the introduction of the incompatible second components, like  $\text{K}^+$  ion in the  $\text{NaNO}_3$  structure or  $\text{Na}^+$  ion in the  $\text{KNO}_3$ . The introduction of ions influenced the order kinetics in a significant way which is related to the equilibrium kinetics in the  $M_0$  system (Ping et al., 2009, pp. 27-36).

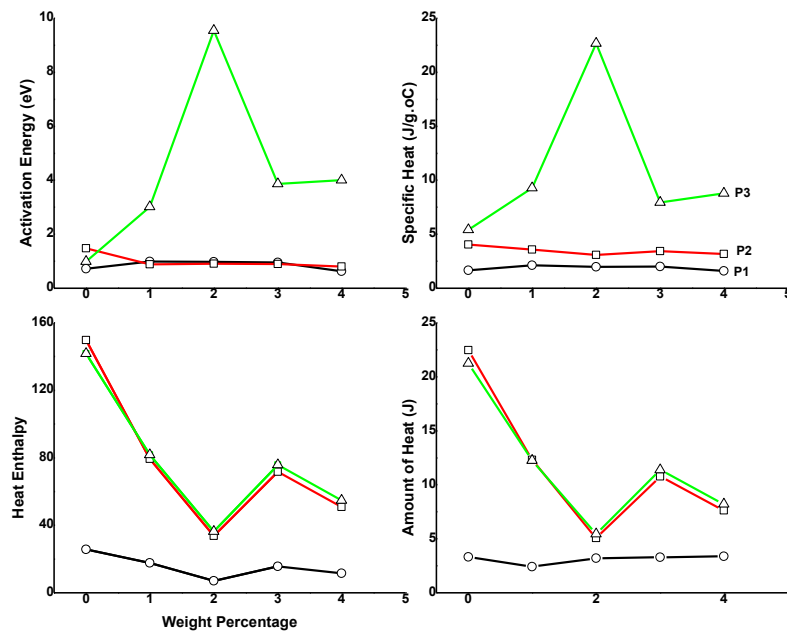


**Figure 3. The Thermal Kinetic Parameters (Activation Energy, Specific Heat, Heat Enthalpy and Amount of Heat) for  $M_{0x}$  System with Different Concentration of Nano Silica**

The changes in the activation energy ( $E_g$ ), the specific heat ( $C_p$ ) and the latent heat ( $\Delta Q$ ) for the different phases ( $P_1$ ,  $P_2$  and  $P_3$ ) in the  $M_{01}$  systems are mainly related to the thermal activation process in this system. These parameters are affected by the concentration percentage of nano-silica and the variation in the strength of  $Na^+$  and  $K^+$  ions bonds in the  $(Na_{0.6}K_{0.4})NO_3$  ( $M_0$ ) system. This variation in the bonds strength plays an important role in the delocalization of charge carried inside the  $M_{0x}$  system. The changes in the latent heat ( $\Delta Q$ ) and ( $C_p$ ) for the phase ( $P_1$ ) are very small, because this phase has a rather low heat for the transformation process. However, in the two phases  $P_2$  and  $P_3$ , the changes in  $\Delta Q$  and  $C_p$  are greater than the phase  $P_1$ , which is mainly related to the large volume variations during the transformation process.

The value of the activation energy in phase ( $P_3$ ) is higher than the values obtained for the phase  $P_2$  and phase  $P_1$ . This is because the ordered parameters in the phase  $P_3$  increase with decreasing the temperature of transformation (liquid-solid). However, the ordered parameters decrease with increasing the temperature in phase ( $P_2$ ) (solid-liquid) phase, i.e., higher disorder, so that the  $E_g$  in phase  $P_3$  is higher than  $P_2$  and  $P_1$  phases (Papon et al., 2002).

The effect of the nano-silica on the thermal properties for the thermal storage  $M_0$  system could be potentially due to the large distribution of the nano-silica per unit volume. This is because the nano-particle has a small diameter and could be more effectively dispersed into the salt  $(Na_{0.6}K_{0.4})NO_3$  and give better pores system and thermal characteristic, that is mainly related to the high specific surface energy in the  $M_0$  system associated with the high surface area of the nano-silica inside the  $M_0$  matrix (Chieruzzi et al., 2013, pp. 448-456).

The obtained results confirmed that the rates of changes in the kinetic and thermo-physical parameters are mainly dependent on the concentration rate of nano-silica inside this system. The results confirmed that the optimum concentration for the thermal storage  $(Na_{0.6}K_{0.4})NO_3$  system is  $x \approx 2\%$  of nano-silica.

### 3.2 Electrical and Thermal Conductivity Measurements

One of the most popular of the nano-silica is mainly related to its good resistance of heat and electricity, so that it has tendency to agglomerate or cluster due to the dominant intermolecular Van der-Waals interaction between the particles. So that the electrical and thermal conductivity of the mixed samples with nano-silica particles mainly depend on the characterization of these nanoparticles and the uniform of dispersion of the nanoparticles in the matrix  $[Na_{0.6}K_{0.4}]NO_3$  (Ning et al., 2009, pp. 518-523).

Figure 3 shows the variation of the electrical conductivity for the system  $M_{01}$  as a function of the temperature. The inset shows the variation of electrical conductivity with the concentration of nano-silica at certain temperature ( $\approx 125^\circ C$ ). From this figure, we can see that the values of electrical conductivity increase with increase the nano-silica up to  $x=2\%$ , and then it decreases with the increase of the nano-silica. This modification enhanced the electrical conduction mechanism inside the  $M_{01}$  system (Chieruzzi et al., 2013, pp. 448-456). The increase in the electrical conductivity up to  $x=2\%$ , may be related the mono dispersion of spherical nano-silica in the matrix  $M_0$  system. Besides that, the increase in the rate of the reorientation process inside the  $M_0$  matrix for the  $K^+$  and  $Na^+$  ion surrounding the  $NO_3^-$  ion group by the effect of temperature on the  $M_{01}$  matrix. However, the decreasing in the electrical conductivity with the increasing of nano-silica after ( $x=2\%$  wt), could be attributed to the reduction in the bond of mobility ions released by the distribution of nano-silica inside the  $M_0$  matrix. It could be also attributed to the effect of the alkalinity degree of nano-silica ratio for the  $M_{01}$  system. Also, the nano-silica has a lower relative density than  $M_0$  system, therefore for given mass replacement from nano-silica into the  $M_0$  system consequently leads to a lower pore volume, due to the size of the nano-silica particles. Beside that the nano-silica is not a good conductor for the electrical properties (Kumar, 2008, pp. 684-687).

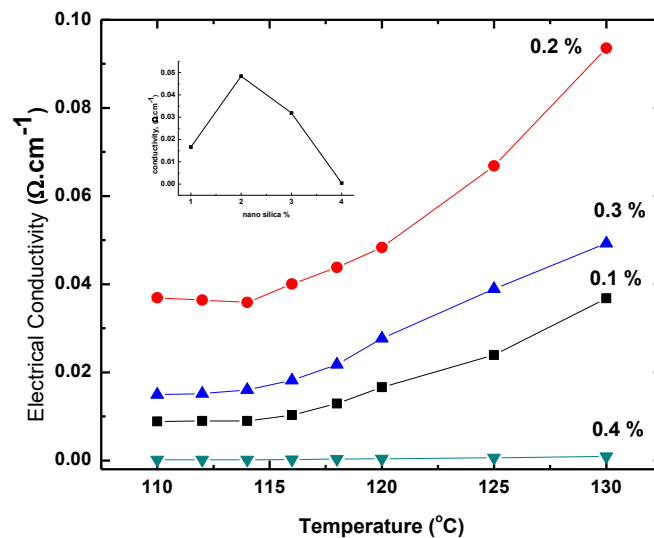


**Figure 4. The Variation of Electrical Conductivity with Temperature for Different Nano-Silica Concentrations in the Solid-Solid Phase**

The activation energies of the  $M_{0x}$  crystal systems are calculated according to the well-known exponential relation (Rysava, 1987, pp. 1015-1021).

The dependence of activation energy on the concentration of nano-silica is shown in Figure 4. It is clear from the figure that there is a minimum value at  $x=2\%$  nano silica. The variation of activation energy is mainly related to the lattice thermal vibration and the formation of polarizability arising from the cationic  $Na^+$  and  $K^+$  ions around the  $(NO_3)^-$  group (Taha, 1989, pp. 341-354).

This process is mainly affected by the temperature of the system and the rate of concentration of nano-silica inside the  $M_0$  matrix system. The modification of activation energy ( $E_g$ ) by the presence of nano silica can be attributed to the appearance of different polaronic and defect levels in the structure of the  $M_{01}$  system (Papon et al., 2002).



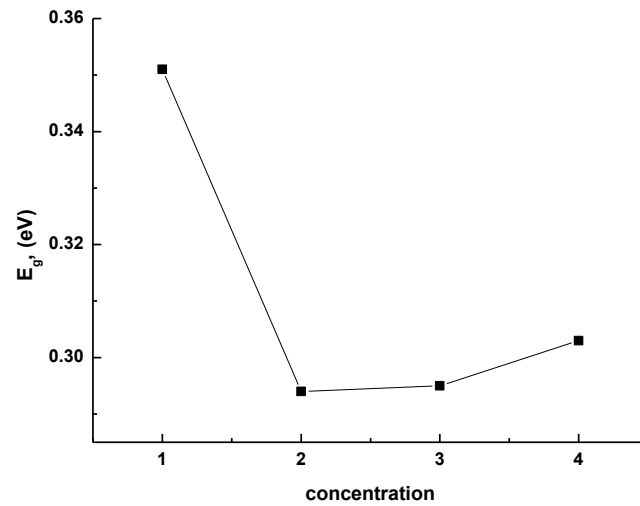


**Figure 5. The Variation of Activation Energy  $E_g$  with Different Concentrations of Nano Silica in the Solid-Solid Phase**

The thermal conductivity ( $k$ ) for the  $M_{0x}$  systems was calculated from the analysis of the DSC thermo-gram curve for the phase  $P_1$  and during heating by using the following relation:

$$k = \frac{qL}{A(T_h - T_l)} \quad (3)$$

Where  $q$  is the heat flow,  $L$  is the thickness,  $A$  is the area,  $(T_h - T_l)$  is the difference between high and low temperature.

The variation of the thermal conductivity  $k$  of the  $M_0$  and  $M_{01}$  systems with the concentration of the nano-silica is shown in Figure 5. It is clear from the figure that thermal the conductivity decreases with the increasing of concentration of the nano-silica and then it reaches a nearly constant value starting at  $x=2\%$  of nano silica.

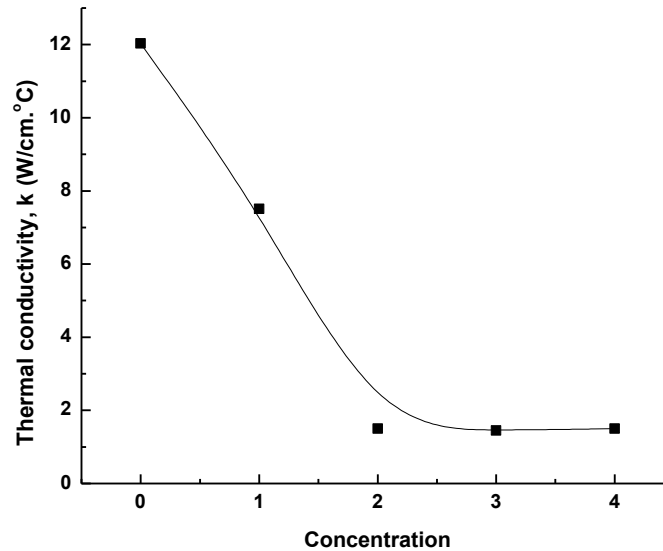


**Figure 6. The Variation of Thermal Conductivity with Different Concentration of Nano-Silica for  $M_{01}$  System in the Solid-Solid Phase**

This indicates that the presence of nano silica increases the thermal resistance to the thermal fluctuations process (Kumar, 2008, pp. 684-687).

It can be said also that the stability of thermal conductivity starting at  $x=2\%$ . This is because the decreasing for the thermal fluctuations leads to decrease in the free energy, i.e., the system become thermally stable (Kumar, 2008, pp. 684-687).

#### 4. Conclusion

The additive nano-silica to the eutectic  $(Na_{0.6}K_{0.4})NO_3$  system bring a new and good additional physical properties to the thermal storage materials, which reasonable to improve the thermal charge and discharge heat energy during the phase changes transformation process. It has been found that the optimum conditions for this additive are satisfied at 2% wt for nano-silica Nano-silicais characterizes by high mechanically stability and act as insulator for heat and electricity. The variation in the thermo-physical properties ( $C_p$ ,  $\Delta H$ ,  $\Delta Q$ , and peak height) for each phase ( $P_1$ ,  $P_2$  and  $P_3$ ) are mainly related to the effect of the nano-silica. It causes also an enhancement in the thermal properties, which is the aim from this work. The thermal analysis measurements indicated that nano-silica has no effect on the transition temperature ( $T_i$ ), which is mainly related to the high stability of solid-solid phase ( $P_1$ ), due to the kinetic hindrance of the disphasic region (Na K) around the  $(NO_3)$  group in the  $M_0$  system. The effect of the nano-silica on the thermal storage media ( $M_0$ ) matrix is mainly related to the reflected modification of the electronic structure of this material. This considerable variation can be attributed to the appearance of different polaronic and defect levels. It has been found that the system  $M_{02}$  whose

nano-silica addition rate of 2 wt%, has the most favorable thermal characteristics. This leads to an improvement in the porosity of the system due to the degree of homogeneity caused by the thermophoresis effect distribution. The distribution of the nano-silica in the  $M_0$  system (thermophoresis effect) makes changes in the porous ratio, due to the high specific area of the nano-silica. This change in the porous system leading to effect on the performance of heating and cooling cycle, beside the rate of melting and freezing for this system.

## References

- Al Sharhani, M. A. S. (2016). *Temperature Dependence of Physical Properties of Some Thermal Storage Materials in Solid Phase* (M.Sc thesis). King Khalied Univeristy, physics department, Faculty of science.
- Bauer, T., Laing D., & Tamme, R. (2010). Overview of PCMs for concentrated solar power in the temperature range 200 to 350°C. *Advances in science and Technology*, 74, 272-278. <https://doi.org/10.4028/www.scientific.net/AST.74.272>
- Berg, R. W., & Kerridge, D. H. (2004). The NaNO<sub>3</sub>/KNO<sub>3</sub> system: The position of the solidus and subsolidus. *Dalton Transactions*, 15, 2224-2229. <https://doi.org/10.1039/b403260h>
- Borul, S. I., & Bergman, A. G. (1954). *Izv. SektoraFiz. Khim. Analiza Inst. Akad. Nauk. SSSR*, 25, 233-238.
- Chen, Y. M., Luo, W., Wang, J., & Huang, J. (2017). Enhanced Thermal Conductivity and Durability of a Paraffin Wax Nanocomposite Based on Carbon-Coated Aluminum Nanoparticles. *J. Phys. Chem. C*, 121(23), 12603-12609. <https://doi.org/10.1021/acs.jpcc.7b02651>
- Chieruzzi, M., Cerritelli, G. F., Miliozzi, A., & Kenny, J. M. (2013). Effect of nanoparticles on heat capacity of nanofluids based on molten salts as PCM for thermal energy storage. *Nanoscale Research Letters*, 8, 448-456. <https://doi.org/10.1186/1556-276X-8-448>
- Dorete, L., Wolf-Dieter, S., Rainer, T., Antje, W., & Stefan, Z. (2012). Advances in thermal energystorage development at the german aerospace center (DLR). *Energy Storage Science and Technology*, 1(1), 13-25.
- Dudda, B., & Shin, D. (2013). Effect of nanoparticles dispersion on specific heat capacity of binary nitrate salt eutectic for cocentrated solar power applications. *International Journal of Thermal Science*, 69, 37-42. <https://doi.org/10.1016/j.ijthermalsci.2013.02.003>
- Farid, M. M., Khudhair, A. M., Razack, S. A. K., & Al-Hallaj, S. (2004). A review on phase change energy storage: Materials and applications. *Energy Conversion and Management*, 45, 1597-1615. <https://doi.org/10.1016/j.enconman.2003.09.015>
- Fredi, G., Dorigato, A., Fambri, L., & Pegoretti, A. (2017). Wax Confinement with Carbon Nanotubes for Phase Changing Epoxy Blends. *Polymers*, 9(9), 405-420. <https://doi.org/10.3390/polym9090405>

- Gaosheng, W., Gang, W., Chao, X., Xing, J., Lijing, X., Xiaoze, D., & Yongping, Y. (2018). Selection principles and thermophysical properties of high temperature phase change materials for thermal energy storage: A review. *Renewable and Sustainable Energy Reviews*, 81(2), 1771-1786.
- Goswami, D. Y., Jotshi, C. K., & Olszewski, M. (1990). Analysis of thermal energy storage in cylindrical PCM capsules embedded in a metal matrix, 25th Intersociety Energy Conversion Engineering Conference. *IECEC Reno, NV, USA* (August 12-17).
- Grant, D. J. W. (2002). Theory and origin of polymorphism. In H. G. Brittain, & D. Marcel (Eds., 2nd ed., pp. 1-34), *Polymorphism in Pharmaceutical solids*. New York.
- Hassan, N., Mariah, B., Francisco, J., Bolivar, O., Marlory, I. R., Xinhai, X., ... Arunachala, M. K. (2019). Recent developments in phase change materials for energy storage applications: A review. *International Journal of Heat and Mass Transfer*, 129, 491-523. <https://doi.org/10.1016/j.ijheatmasstransfer.2018.09.126>
- Hatakeyama, T., & Kanetsuna, H. (1989). Thermal analysis of polymer samples by round robin method: part II factors affecting transition. *Thermochimica Acta*, 138(2), 327-335. [https://doi.org/10.1016/0040-6031\(89\)87269-7](https://doi.org/10.1016/0040-6031(89)87269-7)
- Jeyaseelan, T. R., Azhagesan, N., & Pethurajan, V. (2019). Thermal characterization of NaNO<sub>3</sub>/KNO<sub>3</sub> with different concentrations of Al<sub>2</sub>O<sub>3</sub> and TiO<sub>2</sub> nanoparticles. *Journal of Thermal Analysis and Calorimetry*, 136, 235-242. <https://doi.org/10.1007/s10973-018-7980-6>
- Joel, B. (2008). *Polymorphism in molecular crystal*. UK: Oxford University Press
- Kamimoto, M. (1981). Thermodynamic properties of 50 mole% NaNO<sub>3</sub>-50% KNO<sub>3</sub> (HTS2). *Thermochimica Acta*, 49(2), 319-331. [https://doi.org/10.1016/0040-6031\(81\)80184-0](https://doi.org/10.1016/0040-6031(81)80184-0)
- Kearney, D., Herrmann, U., Nava, P., Kelly, B., Mahoney, R., Pacheco, J., ... Price, H. (2003). Assessment of molten salt heat transfer fluid in a parabolic trough solar field. *J. Sol. Energy Eng.*, 125(2), 170-176. <https://doi.org/10.1115/1.1565087>
- Kumar, G. G., Senthilarasu, S., Lee, D. N., Kim, A. R., Kim, P., Nahm, K. S., ... Elizabeth, R. N., (2008). Synthesis and characterization of aligned SiO<sub>2</sub> nanosphere arrays: Spray method. *Synthetic Metals*, 158(17-18), 684-687. <https://doi.org/10.1016/j.synthmet.2008.04.031>
- Leong, K. Y., Abdul Rahman, M. R., & Gurnathan, B. A. (2019). Nano-enhanced phase change materials: A review of thermo-physical properties, applications and challenges. *Journal of Energy Storage*, 21, 18-31. <https://doi.org/10.1016/j.est.2018.11.008>
- Lin, Y., Alva, G., & Fang, G. (2018). Review on thermal performances and applications of thermal energy storage systems with inorganic phase change materials. *Energy*, 165, 685-708. <https://doi.org/10.1016/j.energy.2018.09.128>
- Lin, Y., Jia, Y., Alva, G., & Fang, G. (2018). Review on thermal conductivity enhancement, thermal properties and applications of phase change materials in thermal energy storage. *Renewable and Sustainable Energy Reviews*, 82, 2730-2742. <https://doi.org/10.1016/j.rser.2017.10.002>

- Lopez, J., Acem, Z., & Del Barrio, E. P. (2010). KNO<sub>3</sub>/NaNO<sub>3</sub>—Graphite materials for thermal energy storage at high temperature: Part II. Phase transition properties. *Applied Thermal engineering*, 30(13), 1586-1593. <https://doi.org/10.1016/j.applthermaleng.2010.03.014>
- Ning, N., Calro, F., Van Duin, A. C. T., & Wales, D. J. (2009). Spontaneous self-assembly of silica nanogases in inorganic framework materials. *J. phys. Chem. C.*, 113(2), 518-523. <https://doi.org/10.1021/jp804528z>
- Papon, P., Leblond, J., & Meijer, P. E. H. (2002). *The physics of phase Transitions*. Springer verlag berlin Heidelberg Germany. <https://doi.org/10.1007/978-3-662-04989-1>
- Ping, W., Harrowell P., Byrne N., & Angell C. A. (2009). Composition dependence of the solid state transitions in NaNO<sub>3</sub>/KNO<sub>3</sub> mixtures. *Thermochimica Acta.*, 486(1), 27-36. <https://doi.org/10.1016/j.tca.2008.12.017>
- Rysava, N., Spasov, T., & Tich, L. (1987). Isothermal DSC method for evaluation of the kinetics of crystallization in the Ge-Sb-S glassy systems. *Journal of Thermal Analysis*, 32, 1015-1021. <https://doi.org/10.1007/BF01905157>
- Shin, D., & Banerjee, D. (2011). Enhancement of specific heat capacity of high-temperature silica-nanofluids synthesized in alkali chloride salt eutectics for solar thermal energy storage applications, *Int. J. Heat Mass. Tran.*, 54(5), 1064-1070. <https://doi.org/10.1016/j.ijheatmasstransfer.2010.11.017>
- Silverman, M. D., & Engel, J. R. (1977). *Survey of Technology for Storage of Thermal Energy in Heat Transfer Salt* (pp. 1-26). US Dep. Commer, ORNL/TM-5682.
- Taha, S., & Tosson, M. (1994). The effect of temperature and phase state on the infrared spectrum of Ba(NO<sub>3</sub>)<sub>2</sub>. *Thermochemica Acta*, 236, 217-226. [https://doi.org/10.1016/0040-6031\(94\)80270-X](https://doi.org/10.1016/0040-6031(94)80270-X)
- Taha, S., Abou-Sehly, A. M., Attia, G., & El-Sharkawy, A. A. (1991). Measurements of thermo-physical properties of KNO<sub>3</sub>. *Thermochemica Acta*, 181, 167-171. [https://doi.org/10.1016/0040-6031\(91\)80421-E](https://doi.org/10.1016/0040-6031(91)80421-E)
- Taha, S., EL-Kabbany, F., & Tosson, M. (1989). Detailed IR study of the phase transition in the system AgNO<sub>3</sub>-Fe(NO<sub>3</sub>)<sub>3</sub>. *Annalen der physic*, 501(5), 341-354. <https://doi.org/10.1002/andp.19895010504>
- Tao, Y. B., & He, Y. L. (2018). A review of phase change material and performance enhancement method for latent heat storage system. *Renewable and Sustainable Energy Reviews*, 93, 245-259. <https://doi.org/10.1016/j.rser.2018.05.028>
- Thirriwg, W. (2006). Paths of Discovery. Pontifical Academy of sciences, Vatican City. *Acta*, 18, 113-121.
- Villada1, C., Bol ívar, F., Jaramillo, F., Castañõ1, J. G., & Echeverr á, F. (2014). Thermal evaluation of molten salts for solar thermal energy storage. *Renewable Energies and Power Quality journal*, 12, 622-625. <https://doi.org/10.24084/repqj12.431>

- Voskresenskaya, N. K. (1970). Handbook of Solid-Liquid Equilibria in Systems of Anhydrous Inorganic Salts. In *Jerusalem* (pp. 431-437). Kete Press.
- Wu, Z. G., & Zhao, C. Y. (2011). Experimental investigations of porous materials in high temperature thermal energy storage systems. *Solar Energy*, 85(7), 1371-1380. <https://doi.org/10.1016/j.solener.2011.03.021>
- Xiao, J., Huang, J., Zhu, P., Wang, C. H., & Li, X. (2014). Preparation, characterization and thermal properties of binary nitrate salts/expanded graphite as a composite phase change material. *Thermochimica Acta*, 587, 52-58. <https://doi.org/10.1016/j.tca.2014.04.021>
- Xiao, X., Zhang, P., & Li, M. (2015). Experimental and numerical study of heat transfer performance of nitrate/expanded graphite composite PCM for solar energy storage. *Energy Conversion and Management*, 105, 272-284. <https://doi.org/10.1016/j.enconman.2015.07.074>
- Xu, B., Li, P. W., & Cholik, C. (2015). Application of phase change materials for thermal energy storage in concentrated solar thermal power plants: A review to recent developments. *Applied Energy*, 160, 286-307. <https://doi.org/10.1016/j.apenergy.2015.09.016>
- Zhang, X., Tian, J., Xu, K., & Gao, Y. (2003). Thermodynamic Evaluation of Phase Equilibria in  $\text{NaNO}_3\text{-KNO}_3$  System. *Journal of Phase Equilibria*, 24(5), 441-446. <https://doi.org/10.1361/105497103770330091>
- Zhao, Y. J., Wang, R. Z., Wang, L. W., & Yu, N. (2014). Development of highly conductive  $\text{KNO}_3/\text{NaNO}_3$  composite for TES (thermal energy storage). *Energy*, 70, 272-277. <https://doi.org/10.1016/j.energy.2014.03.127>